Research Article Vol. 6, No. 1 / January 2019 / Optica 56

Ultrafast broadband circular dichroism in the deep ultraviolet

Malte Oppermann,[1,*] Benjamin Bauer,[1] Thomas Rossi,[1] Francesco Zinna,[2] Jan Helbing,[3] Jérôme Lacour,[2] and Majed Chergui[1]

[1]Laboratoire de Spectroscopie Ultrarapide and Lausanne Centre for Ultrafast Science (LACUS), École Polytechnique Fédérale de Lausanne, ISIC-FSB, CH-1015 Lausanne, Switzerland
[2]Département de chimie organique, Université de Genève, Quai Ernest Ansermet 30, 1211 Genève 4, Switzerland
[3]Institut für Chemie, Universität Zürich, Winterthurerstrasse 190, 8057 Zürich, Switzerland
*Corresponding author: malte.oppermann@epfl.ch

Received 8 August 2018; revised 17 October 2018; accepted 9 November 2018 (Doc. ID 341887); published 10 January 2019

The measurement of chirality and its temporal evolution are crucial for the understanding of a large range of biological functions and chemical reactions. Steady-state circular dichroism (CD) is a standard analytical tool for measuring chirality in chemistry and biology. Nevertheless, its push into the ultrafast time domain and in the deep-ultraviolet has remained a challenge, with only some isolated reports of subnanosecond CD. Here, we present a broadband time-resolved CD spectrometer in the deep ultraviolet (UV) spectral range with femtosecond time resolution. The setup employs a photoelastic modulator to achieve shot-to-shot polarization switching of a 20 kHz pulse train of broadband femtosecond deep-UV pulses (250–370 nm). The resulting sequence of alternating left- and right-circularly polarized probe pulses is employed in a pump-probe scheme with shot-to-shot dispersive detection and thus allows for the acquisition of broadband CD spectra of ground- and excited-state species. Through polarization scrambling of the probe pulses prior to detection, artifact-free static and transient CD spectra of enantiopure $[Ru(bpy)_3]^{2+}$ are successfully recorded with a sensitivity of $<2 \times 10^{-5}$ OD (≈0.7 mdeg). Due to its broadband deep-UV detection with unprecedented sensitivity, the measurement of ultrafast chirality changes in biological systems with amino-acid residues and peptides and of DNA oligomers is now feasible.

https://doi.org/10.1364/OPTICA.6.000056

1. INTRODUCTION

Circular dichroism (CD) denotes the difference in absorption of left- and right-handed circularly polarized light in chiral molecular systems. In the deep-UV range (<300 nm), it is sensitive to the coupling and thus the spatial arrangement of electronic transition dipoles of amino acids and nucleotides. For this reason, static CD spectroscopy has become an established tool in analytical biochemistry and chemistry, where it is typically used to determine the secondary structure of proteins and DNA systems in the condensed phase [1]. Consequently, time-resolved CD spectroscopy (TRCD) is a promising experimental technique that is sensitive to changes in biomolecular configuration as a function of time, combining the time-dependent electronic information provided by traditional transient absorption (TA) spectroscopy with the structural information encoded in the chirality of molecular systems. CD spectroscopy does not provide the atomic resolution possible with other structurally sensitive spectroscopic techniques such as x-ray absorption and crystallography and nuclear magnetic resonance (NMR) spectroscopy, yet typically displays superior data acquisition (DAQ) speeds combined with tabletop instrumentation. Furthermore, its comparatively low sample concentration requirements and straightforward application to condensed phase systems with few restrictions on the solvent choice are ideally suited for the study of biological systems under physiological conditions. Most importantly, however, CD spectroscopy is a technique with structural sensitivity in the optical spectral range. With the use of pulsed ultrafast laser technology in a pump-probe scheme, it is now possible to measure transient chirality changes on time scales spanning from the nano- [2] to the femtosecond regime [3]. CD spectroscopy therefore offers a direct, nonempirical route to follow structural changes of molecular systems on the shortest time scales currently explored in molecular dynamics research.

Despite its many advantages, three technical challenges have slowed progress for the experimental implementation of TRCD. First, transient CD signals are typically at least an order of magnitude lower than typical static CD signals. TRCD measurements thus require a sensitivity on the order of 1 mdeg in the commonly employed units of ellipticity, which corresponds to an absorptivity of $\approx 3 \times 10^{-5}$ OD. Such sensitivities have only recently been achieved in the visible (>400 nm) spectral regime [4,5]. Second, broadband detection is extremely difficult due to the polarization sensitivity of dispersive and reflective optics, which easily distorts static CD spectra [6,7]. This has limited commercial static CD spectropolarimeters and many TRCD setups to narrowband detection schemes [3,5,8], thus requiring probe wavelength scanning with increased DAQ

times. Notable exceptions now exist in the visible spectral range [4,9,10]. Third, most biologically relevant chromophores are located in the deep UV, which thus requires both a broadband, intense laser pulse source and a suitably broadband polarization modulation scheme covering this spectral regime. Yet despite the existence of sufficiently broadband sources [11] and recent developments in laser pulse polarization management [12,13], no broadband TRCD setup in the deep UV has been reported thus far.

We now address all of the above challenges by combining a femtosecond broadband deep-UV source at a high repetition rate with broadband shot-to-shot polarization state switching via a photoelastic modulator (PEM). In addition, our setup minimizes polarization artifacts through polarization scrambling prior to broadband dispersive detection.

2. EXPERIMENTAL SETUP

The laser setup for generating the deep-UV probe pulses has been described in detail elsewhere [14,15]. Briefly, a customized cryogenic Ti:Sapphire amplifier, with an exceptional shot-to-shot stability of 0.1% root mean square, pumps a commercial noncollinear optical parametric amplifier at 20 kHz. The broadband visible femtosecond pulses are achromatically doubled in a thin beta barium borate (BBO) crystal [11] covering the 250–370 nm range. The polarization state of these probe pulses is switched on a shot-to-shot basis via a PEM. This resonant optical retardation device (I/FS50, Hinds Instruments) modulates the polarization of the transmitted light at 50 kHz via the periodic stress-induced birefringence in a 6 mm thick fused silica block. The modulation amplitude thus determines the maximum retardation that is achieved with opposite handedness at the maximum and minimum of the modulation cycle. Through a quasi-synchronization of the amplifier with the PEM [16], the probe pulses are spaced by 2.5 modulation periods, such that the appropriate amplifier delay and modulation amplitude generate a probe pulse train with circular polarization states of alternating handedness. While the probe pulse ellipticity is wavelength-dependent and thus circular only on average, this scheme ensures a high degree of symmetry of the left- and right-handed pulses over their entire spectral range. In this case, the CD measured at a probe wavelength λ is approximately proportional to $2\sin(\theta)\cos(\theta)$, where θ denotes the PEM's retardation at this wavelength [17]. For very large probe bandwidths, the wavelength-dependent retardation should thus be measured separately [17] and employed as a calibration factor in the measured CD. However, for a fused silica PEM set to $\theta = \pi/4$ at $\lambda = 300$ nm, the correction is expected to be <5% in the 250–370 nm region covered here. Indeed, we could well reproduce static CD spectra in this wavelength range without any scaling, as shown in the results section of this paper. It should also be noted that compared to other retardation devices, especially Pockels cells, the PEM has a very large acceptance angle, which thus offers broadband polarization switching at a high repetition rate without the need for complex alignment procedures [18].

Figure 1 displays the optical scheme of the TRCD setup. Before polarization modulation, the deep-UV probe beam is split via a 1 mm thick reflective neutral density filter (BS in Fig. 1) with an optical density of 0.3 OD. The reflected beam is used for multichannel referencing and is detected on a separate chip in the same spectrometer as the probe beam. The transmitted probe is focused with a 20 cm focal length off-axis parabolic mirror (labeled OAP and represented by a lens in Fig. 1) through a

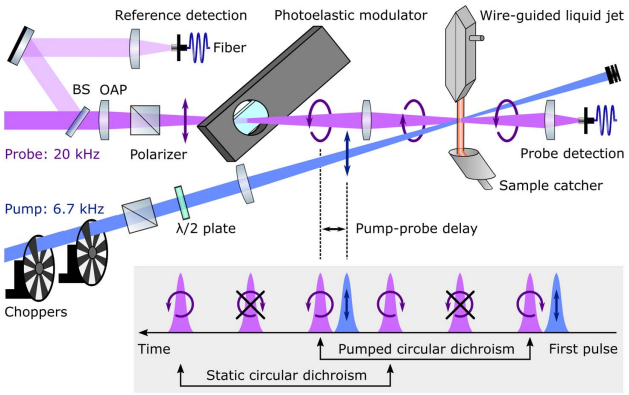

Fig. 1. Schematic drawing of the time-resolved CD setup, where the probe polarization is switched by a PEM. The inset displays the sequence of six consecutive probe pulses necessary to obtain a transient CD spectrum.

Glan-Laser polarizer. With a measured focal spot size of 83 μm ($1/e^2$), the PEM is placed within the Rayleigh range of the probe focus and positioned at 45° with respect to the incident vertical probe polarization. Focusing through the PEM has two advantages. First, it minimizes its modulation-dependent lensing effect [19]. Second, it is well known that the PEM has a residual static birefringence that is inhomogeneously distributed over the vibrating fused silica (FS) block [20]. As a result, the effective birefringence of the PEM may be reduced to a sufficiently small level by focusing the probe beam through a spot on the FS crystal with minimal residual birefringence. Finally, the thickness modulation of the PEM crystal acts as a source for air density fluctuations (acoustic wave), which are synchronized with the polarization modulation. The resulting differences in beam pointing are large enough to spectrally distort the baseline of the static CD measurement to values between 0.5 and 1.0 mOD, which is on the order of moderate CD signals. Due to the dynamic nature of the acoustic wave, these distortions cannot be subtracted reliably as a background. Nevertheless, this effect can be minimized by tightly enclosing the PEM in a box with pinholes for the transmitted probe beam that are only slightly larger than the beam diameter.

After the PEM, the diverging probe beam is refocused with a 15 cm focal length FS lens through a 200 μm thick wire-guided liquid jet (design adapted from [21]) with a focal spot size of about 80 μm full width at half-maximum (FWHM). The jet has a closed-loop sample flow system and employs a syringe pump to compensate for solvent evaporation. Compared to sample cells, the jet is free of birefringence and can support much higher pump intensities, which is advantageous for increasing TRCD signals. The transmitted probe light is coupled into a 400 μm diameter multimode fiber with an FS lens. Dispersive shot-to-shot detection is achieved via a fiber-coupled imaging spectrograph, equipped with a double-array complementary metal-oxide-semiconductor (CMOS) detector. The second chip is used to record the reference spectrum for correcting the spectral intensity fluctuations of the probe. Crucially, the long multimode fiber efficiently scrambles the probe polarization before its dispersive detection. The fiber thus removes the polarizing effect of the spectrometer optics and minimizes the setup's sensitivity to the birefringence of the employed transmissive optics. This allows for the acquisition of artifact-free, spectrally resolved CD spectra.

The sample is photoexcited with a femtosecond pump pulse that is focused to a spot size of about 200 μm and crosses the probe beam at an angle of about 10°. The pump is derived from the harmonically doubled (400 nm) or tripled (266 nm) output of the Ti:Sapphire amplifier, and its linear polarization is cleaned with a Glan-Laser polarizer. A zero-order half-wave plate ($\lambda/2$) is then used to rotate its polarization. Two optical choppers reduce the pump's repetition rate to a third of that of the probe (6.67 kHz), such that the time between consecutive pump shots is constant. The inset of Fig. 1 displays the resulting sequence of six consecutive probe pulses that are required to obtain a transient CD spectrum. The difference of the left- (LCP) and right-handed circularly polarized (RCP) probe pulses that interact with a pumped sample volume after a variable pump-probe delay results in a CD spectrum of a photoexcited sample (pumped CD). The respective probe shots that follow are discarded (crossed in the figure), and the static CD is obtained as the difference of the remaining LCP and RCP probe shots interacting with a ground-state sample volume. A TRCD spectrum is then obtained by subtracting the static from the pumped CD. While reducing the duty cycle of the measurement, the symmetry of this six-pulse sequence is necessary to obtain artifact-free transient CD spectra. An alternative scheme where two consecutive probe pulse are pumped, for example, did not lead to satisfactory results. Possible reasons for this may be incomplete sample exchange, residual chopping errors, or electronic memory in the detection system.

In order to determine the instrument response function (IRF) of this setup, one may also view the pulse sequence as two consecutive TA measurements with circularly polarized probe pulses of opposite handedness. The IRF was thus obtained for both probe polarization states via the two-photon absorption signal in ethanol with a 266 nm pump pulse. Gaussian fits to the resulting time traces at each detector pixel gave an average FWHM of 500 fs across the probe spectrum. For each probe polarization state, the obtained fit parameters, such as temporal width and pump-probe overlap, agreed within their respective error ranges. The relatively long IRF is caused by the dispersion of the polarizer and the PEM in the probe beam path, which add up to a total thickness of about 1.6 cm. This also causes a large group velocity dispersion (GVD) of the probe pulse, which is about 8 ps. While an improved pulse compression is possible in the future [11], the GVD is simply corrected in the data analysis at present, as is customary in TA experiments and limited in time resolution only by the measured IRF.

The pump induces an anisotropic distribution of excited molecules in the laboratory frame with a lifetime limited by rotational diffusion. This transient birefringence effect is expected to lead to strong TRCD artifacts, as suggested by CD measurements of oriented samples [22]. With linear probe polarization in a TA experiment, the polarization angle with a linear pump can be set to eliminate this effect in the recorded spectral kinetics. This so-called magic angle condition is more complex for TRCD as the circular probe polarization breaks the cylindrical symmetry of a linear probe [23] and should take quadrupolar light-molecule interactions into account [24,25]. Furthermore, any residual birefringence in the setup, combined with any remaining polarization sensitivity of the dispersive spectrometer after the scrambling of the probe polarization, will translate the linear dichroism of the pump-induced sample anisotropy into an artificial TRCD signal [7,26]. In this context, nanosecond TRCD experiments

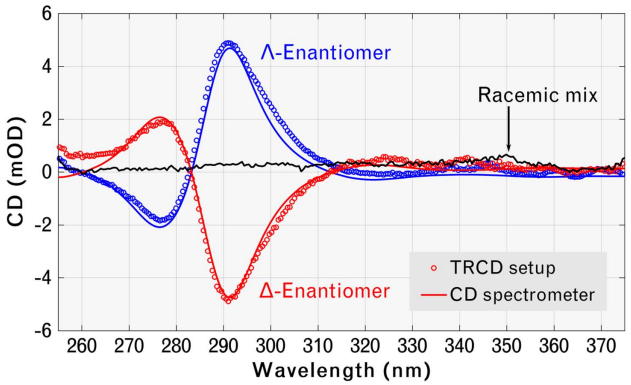

Fig. 2. Static CD spectra of both enantiomers of $[Ru(bpy)_3]^{2+}$ and the corresponding racemic sample in 1.0 mM aqueous solution and their comparison with CD spectra obtained with a commercial CD spectrometer.

combined with theoretical modeling have shown that one can expect this effect to be suppressed when the pump polarization is parallel or perpendicular to the effective polarization axis of the spectrometer [7]. However, in the present setup, it is difficult to precisely determine the effective polarization axis of the dispersive spectrometer and the residual ellipticity of the probe light that enters it. The magic angle condition is therefore determined experimentally *in situ*, prior to an experiment. For this, the TRCD signal of a suitable achiral or racemic sample is measured as a function of the pump polarization angle. In this setup, pump-induced artifacts are consistently minimized between 5° and 15° near parallel and perpendicular pump polarization with respect to the input probe polarization prior to its modulation.

In order to evaluate the performance of the spectrometer, a first batch of enantiomerically pure samples of $[Ru(bpy)_3]^{2+}$ with Cl counter ions were synthesized, following the procedure described in Refs. [27,28]. A second batch of the ruthenium tris(bipyridil) complex of target was obtained in single enantiomeric form using a chiral anion-mediated approach [29,30]. Lipophilic hexacoordinated phosphorus(V) TRISPHAT anions, abbreviated TT [31,32], were added to racemic solutions of $[Ru(bpy)_3](PF_6)_2$, and the resulting diastereomeric complexes were separated by chromatography over silica gel (CH_2Cl_2 as eluent) [33–35]. Then, in a new development, isolated salts $[\Delta - Ru(bpy)_3][\Delta - TT]_2$ and $[\Lambda - Ru(bpy)_3][\Delta - TT]_2$ were transformed into enantiomeric $[\Delta - Ru(bpy)_3](PF_6)_2$ and $[\Lambda - Ru(bpy)_3](PF_6)_2$ (ee >96%) by first extractions in aqueous layers with $[nHex_4N]$ [Br] as phase transfer agent and precipitations of the hexafluorophosphate salts with saturated solutions of KPF_6. Except for different solubilities in water, both sample batches displayed identical static absorption and CD spectra and were thus used interchangeably. Racemic samples were directly prepared from commercially available racemic $[Ru(bpy)_3]^{2+}$ salt. The Δ- and Λ-enantiomers display strong CD bands in the region between 260 and 310 nm, which originate from the excitonic coupling of the long-axis transition dipole moments on the three bipyridine ligands [36].

3. RESULTS

Figure 2 displays the static CD spectra of both enantiomers and the racemic sample in a 1.0 mM aqueous solution acquired with the TRCD setup. For comparison, the CD spectra of the

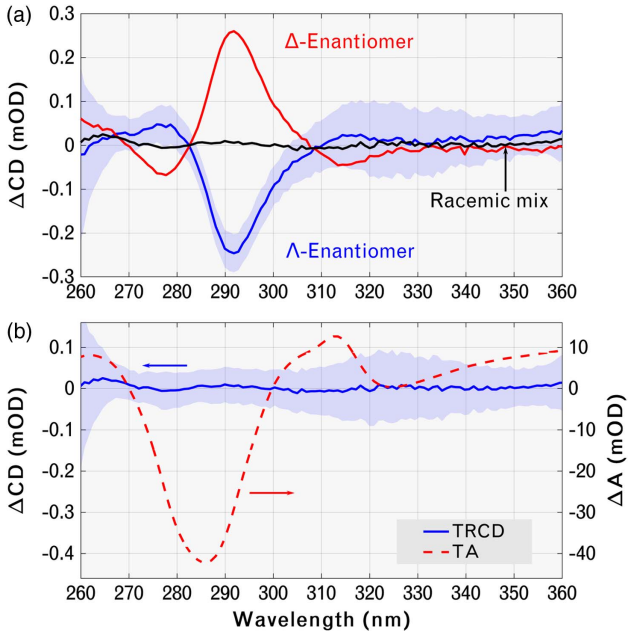

Fig. 3. (a) Time-resolved CD spectra of both enantiomers of $[Ru(bpy)_3]^{2+}$ and the corresponding racemic sample in 0.4 mM aqueous solution, photoexcited with a 400 nm pulse at 50 ps pump-probe delay. The shaded area denotes one standard deviation. (b) TRCD of the racemic sample with the corresponding TA spectrum.

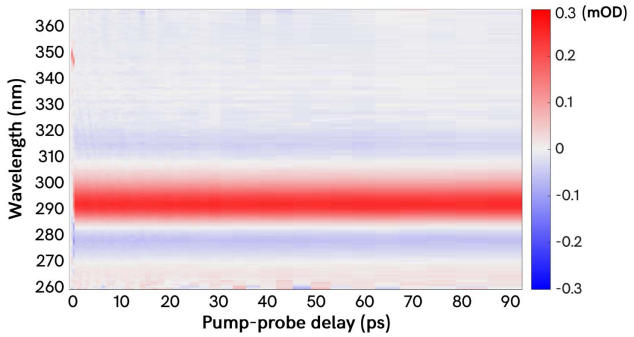

Fig. 4. Time-wavelength TRCD map of Δ – $[Ru(bpy)_3]^{2+}$ in 0.4 mM aqueous solution, photoexcited with a 400 nm pulse.

enantiomers recorded with a commercial CD spectrometer (Jasco J-1100) are displayed as well. The CD spectrum of the racemic sample demonstrates a baseline uncertainty of about 0.2 mOD for its static CD acquisition. Within this range, an excellent qualitative agreement is achieved between our new laser-based setup and the commercial instrument. Quantitatively, minor discrepancies can be observed in the region <265 nm in the case of the Δ- and around 275 nm and in the region 300 to 315 nm for the Λ-enantiomer. Just like the small distortions of the baseline (racemic mix), these must be attributed to slight asymmetries of the circular polarization states caused by the birefringence of the lenses and the PEM [17] and indicate the limit of the polarization scrambling prior to detection. Generally, regions of maximum distortion are sensitive to the spot where the probe beam passes the PEM and can be shifted through the alignment of the instrument.

For the TRCD spectra, the samples are pumped by 400 nm pulses with an estimated peak fluence of 2 mJ cm^{-2}. The associated metal-to-ligand charge transfer (MLCT) transition in $[Ru(bpy)_3]^{2+}$ results in an ultrafast charge localization on one of the ligands, which thus reduces the excitonic coupling of the ligand-centered transition dipoles [37–39]. As in TA measurements, the resulting CD bleach has a negative sign, such that the TRCD spectrum has inverted signs with respect to the static CD spectrum. The corresponding TRCD signal for each enantiomer is displayed in part (a) of Fig. 3 at a fixed pump-probe delay of 50 ps. The spectra of the enantiomers were scaled by their corresponding static CD amplitudes to account for differences in sample concentration and jet thickness. The spectra display an excellent symmetry, with the respective shaded areas indicating the measurement precision as one standard deviation (1σ). In addition, part (b) of Fig. 3 displays the TRCD signal of the racemic mix together with the TA signal of the same measurement. The TRCD signal indicates a baseline uncertainty and thus sensitivity <0.02 mOD, which demonstrates that pump-induced polarization artifacts are successfully minimized in this setup. This is especially noteworthy, given that such artifacts scale with the measured TA amplitude, which is more than 3 orders of magnitude larger than the obtained baseline uncertainty. The displayed noise level with $1\sigma < 1 \times 10^{-4}$ OD was achieved by averaging over a total of 1.5×10^7 laser shots, which corresponds to approximately 15 min of DAQ time. Its spectral dependence is mostly due to a variation of spectral intensity across the probe spectrum. It is worth noting that the resulting sensitivity represents a significant improvement compared to previously reported broadband femtosecond TRCD setups in the visible spectral regime [4], especially considering the added noise from the generation of the deep-UV probe continuum via achromatic frequency doubling.

Figure 4 then displays a time-wavelength TRCD map of Δ – $[Ru(bpy)_3]^{2+}$ in 0.4 mM aqueous solution under the same pumping conditions as in Fig. 3. The data are corrected for GVD of the probe pulse, and each time step corresponds to an average of about 1×10^7 laser shots. The TRCD signal rises instantaneously within the time resolution of the setup and remains constant within the sampled time window. Both observations are consistent with the reported ultrafast charge localization dynamics and lifetime of the associated MLCT state of such complexes [38,39].

4. CONCLUSION

We report the first time-resolved femtosecond CD setup that combines shot-to-shot broadband detection in the deep-UV regime with artifact-free acquisition of static and transient CD spectra with a sensitivity $<2 \times 10^{-5}$ OD. This represents a significant advance in the field of time-resolved chiral spectroscopy that promises important new insights into the structural dynamics of biologically relevant UV chromophores such as amino-acid residues in proteins and nucleotides in DNA oligomers.

Funding. Deutscher Akademischer Austauschdienst (DAAD); Schweizerischer Nationalfonds zur Förderung der Wissenschaftlichen Forschung (SNF) (NCCR-MUST).

Acknowledgment. The authors thank F. van Mourik for technical support and advice. Many thanks also go to M. Asif and F. Freymond for their assistance and to Professor C. Heinis

and Dr. X. Kong at EPFL for support and access to a static CD spectrometer.

REFERENCES

1. G. D. Fasman, ed., *Circular Dichroism and the Conformational Analysis of Biomolecules*, 1996th ed. (Springer, 1996).
2. R. A. Goldbeck, D. B. Kim-Shapiro, and D. S. Kliger, "Fast natural and magnetic circular dichroism spectroscopy," Annu. Rev. Phys. Chem. **48**, 453–479 (1997).
3. J. Meyer-Ilse, D. Akimov, and B. Dietzek, "Recent advances in ultrafast time-resolved chirality measurements: perspective and outlook: ultrafast transient molecular chirality," Laser Photon. Rev. **7**, 495–505 (2013).
4. K. Hiramatsu and T. Nagata, "Communication: broadband and ultrasensitive femtosecond time-resolved circular dichroism spectroscopy," J. Chem. Phys. **143**, 121102 (2015).
5. V. Stadnytskyi, G. S. Orf, R. E. Blankenship, and S. Savikhin, "Near shot-noise limited time-resolved circular dichroism pump-probe spectrometer," Rev. Sci. Instrum. **89**, 033104 (2018).
6. X. Xie and J. D. Simon, "Picosecond time-resolved circular dichroism spectroscopy: experimental details and applications," Rev. Sci. Instrum. **60**, 2614–2627 (1989).
7. S. C. Bjorling, R. A. Goldbeck, S. J. Milder, C. E. Randall, J. W. Lewis, and D. S. Kliger, "Analysis of optical artifacts in ellipsometric measurements of time-resolved circular dichroism," J. Phys. Chem. **95**, 4685–4694 (1991).
8. C. Niezborala and F. Hache, "Measuring the dynamics of circular dichroism in a pump-probe experiment with a Babinet-Soleil compensator," J. Opt. Soc. Am. B **23**, 2418–2424 (2006).
9. L. Mangot, G. Taupier, M. Romeo, A. Boeglin, O. Cregut, and K. D. H. Dorkenoo, "Broadband transient dichroism spectroscopy in chiral molecules," Opt. Lett. **35**, 381–383 (2010).
10. A. Trifonov, I. Buchvarov, A. Lohr, F. Würthner, and T. Fiebig, "Broadband femtosecond circular dichroism spectrometer with white-light polarization control," Rev. Sci. Instrum. **81**, 043104 (2010).
11. P. Baum, S. Lochbrunner, and E. Riedle, "Tunable sub-10-fs ultraviolet pulses generated by achromatic frequency doubling," Opt. Lett. **29**, 1686–1688 (2004).
12. A. Steinbacher, H. Hildenbrand, S. Schott, J. Buback, M. Schmid, P. Nuernberger, and T. Brixner, "Generating laser-pulse enantiomers," Opt. Express **25**, 21735–21752 (2017).
13. F. Preda, A. Perri, J. Réhault, B. Dutta, J. Helbing, G. Cerullo, and D. Polli, "Time-domain measurement of optical activity by an ultrastable common-path interferometer," Opt. Lett. **43**, 1882–1885 (2018).
14. G. Auböck, C. Consani, F. V. Mourik, and M. Chergui, "Ultrabroadband femtosecond two-dimensional ultraviolet transient absorption," Opt. Lett. **37**, 2337–2339 (2012).
15. G. Auböck, C. Consani, R. Monni, A. Cannizzo, F. van Mourik, and M. Chergui, "Femtosecond pump/supercontinuum-probe setup with 20 kHz repetition rate," Rev. Sci. Instrum. **83**, 093105 (2012).
16. M. Bonmarin and J. Helbing, "Polarization control of ultrashort mid-IR laser pulses for transient vibrational circular dichroism measurements," Chirality **21**, E298–E306 (2009).
17. J. Helbing and M. Bonmarin, "Vibrational circular dichroism signal enhancement using self-heterodyning with elliptically polarized laser pulses," J. Chem. Phys. **131**, 174507 (2009).
18. T. Dartigalongue and F. Hache, "Precise alignment of a longitudinal Pockels cell for time-resolved circular dichroism experiments," J. Opt. Soc. Am. B **20**, 1780–1787 (2003).
19. B. Dutta and J. Helbing, "Optimized interferometric setup for chiral and achiral ultrafast IR spectroscopy," Opt. Express **23**, 16449–16465 (2015).
20. B. Wang, E. Hinds, and E. Krivoy, "Basic optical properties of the photoelastic modulator part II: residual birefringence in the optical element," Proc. SPIE **7461**, 746110 (2009).
21. A. Picchiotti, V. I. Prokhorenko, and R. J. D. Miller, "A closed-loop pump-driven wire-guided flow jet for ultrafast spectroscopy of liquid samples," Rev. Sci. Instrum. **86**, 093105 (2015).
22. A. Davidsson, B. Nordén, and S. Seth, "Measurement of oriented circular dichroism," Chem. Phys. Lett. **70**, 313–316 (1980).
23. S. Schott, A. Steinbacher, J. Buback, P. Nuernberger, and T. Brixner, "Generalized magic angle for time-resolved spectroscopy with laser pulses of arbitrary ellipticity," J. Phys. B **47**, 124014 (2014).
24. D. Che, R. A. Goldbeck, and D. S. Kliger, "Theory of natural circular dichroism in molecules oriented by photoselection," J. Chem. Phys. **100**, 8602–8613 (1994).
25. M. Cho, "Two-dimensional circularly polarized pump-probe spectroscopy," J. Chem. Phys. **119**, 7003–7016 (2003).
26. X. Xie and J. D. Simon, "Picosecond circular dichroism spectroscopy: a Jones matrix analysis," J. Opt. Soc. Am. B **7**, 1673–1684 (1990).
27. V. Joshi and P. K. Ghosh, "Spectral evidence of spontaneous racemic and pseudoracemic interactions between optically active poly(pyridyl) metal chelates adsorbed on smectite clays," J. Am. Chem. Soc. **111**, 5604–5612 (1989).
28. R. Puttreddy, J. A. Hutchison, Y. Gorodetski, J. Harrowfield, and K. Rissanen, "Enantiomer separation of tris(2, 2-bipyridine)ruthenium(II): interaction of a D3-symmetric cation with a C2-symmetric anion," Cryst. Growth Des. **15**, 1559–1563 (2015).
29. J. Lacour and D. Moraleda, "Chiral anion-mediated asymmetric ion pairing chemistry," Chem. Commun. **46**, 7073–7089 (2009).
30. O. Maury, J. Lacour, and H. L. Bozec, "Diastereoselective homochiral self-assembly between anions and cation in solution," Eur. J. Inorg. Chem. **2001**, 201–204 (2001).
31. J. Lacour, C. Ginglinger, C. Grivet, and G. Bernardinelli, "Synthesis and resolution of the configurationally stable tris(tetrachlorobenzenediolato) phosphate(V) ion," Angew. Chem. Int. Ed. **36**, 608–610 (1997).
32. F. Favarger, C. Goujon-Ginglinger, D. Monchaud, and J. Lacour, "Large-scale synthesis and resolution of TRISPHAT [tris(tetrachlorobenzenediolato) phosphate(V)] anion," J. Org. Chem. **69**, 8521–8524 (2004).
33. J. Lacour, S. Torche-Haldimann, and J. J. Jodry, "Ion pair chromatographic resolution of tris(diimine)ruthenium(ii) complexes using TRISPHAT anions as resolving agents," Chem. Commun. **0**, 1733–1734 (1998).
34. D. Monchaud, J. J. Jodry, D. Pomeranc, V. Heitz, J.-C. Chambron, J.-P. Sauvage, and J. Lacour, "Ion-pair-mediated asymmetric synthesis of a configurationally stable mononuclear tris(diimine)-iron(II) complex," Angew. Chem. Int. Ed. **41**, 2423–2425 (2002).
35. M. G. N. Reddy, R. Ballesteros Garrido, J. Lacour, and S. Caldarelli, "Determination of Labile chiral supramolecular ion pairs by chromatographic NMR spectroscopy," Angew. Chem. Int. Ed. **52**, 3255–3258 (2013).
36. B. Bosnich, "Application of exciton theory to the determination of the absolute configurations of inorganic complexes," Acc. Chem. Res. **2**, 266–273 (1969).
37. C. Niezborala and F. Hache, "Excited-state absorption and circular dichroism of ruthenium(II) tris(phenanthroline) in the ultraviolet region," J. Phys. Chem. A **111**, 7732–7735 (2007).
38. D. H. Oh and S. G. Boxer, "Stark effect spectra of Ru(diimine)32+ complexes," J. Am. Chem. Soc. **111**, 1130–1131 (1989).
39. A. Cannizzo, F. V. Mourik, W. Gawelda, G. Zgrablic, C. Bressler, and M. Chergui, "Broadband femtosecond fluorescence spectroscopy of $[Ru(bpy)_3]^{2+}$," Angew. Chem. **118**, 3246–3248 (2006).